The merger fraction evolution up to $z \sim 1$

Carlos López-Sanjuan, Marc Balcells, Pablo G. Pérez-González, Guillermo Barro, César Enrique García-Dabó, Jesús Gallego, and Jaime Zamorano

Abstract We present results on the disk-disk major merger fraction evolution up to $z \sim 1$ in SPITZER/IRAC selected samples in the GOODS-S field. We pick as merger remnants sources with high asymmetry (A). We take into account the experimental errors in photometric redshift and index A, that tend to overestimate the merger fraction, by maximum likelihood techniques, and avoid the loss of information with redshift (degradation of spatial resolution and cosmological dimming) with redshift by artificially redshifting all sources to a representative redshift, $z_{\rm d} = 1$.

We define absolute B-band and mass selected samples, for which we obtain a very different merger fraction evolution: $f_{\rm m}^{\rm mph}(z, M_B \leq -20) = 0.013(1+z)^{1.8}$, while $f_{\rm m}^{\rm mph}(z, M_\star > 10^{10}\ M_\odot) = 0.001(1+z)^{5.4}$. These results implies that only $\sim$20%/8% of today's $M_B \leq -20/M_\star > 10^{10}\ M_\odot$ galaxies have undergone a disk-disk major merger since $z = 1$. Combined with high redshift data in the literature, we expect $1.2^{+0.4}_{-0.3}$ disk-disk major mergers since $z \sim 3$ for $M_\star > 10^{10} M_\odot$ galaxies, with almost all the merger activity before $z = 1$.

Carlos López-Sanjuan · Marc Balcells
Instituto de Astrofísica de Canarias, Calle Vía Láctea s/n, E-38200, La Laguna, Tenerife, Spain. e-mail: clsj@iac.es

Pablo G. Pérez-González · Guillermo Barro · Jesús Gallego · Jaime Zamorano
Departamento de Astrofísica y Ciencias de la Atmósfera, Facultad de C.C. Físicas, Universidad Complutense de Madrid, E-28040 Madrid, Spain

César Enrique García-Dabó
European South Observatory, Karl-Schwarzschild-Strasse 2, D-85748 Garching, Germany

1 Introduction

It is well known that more massive galaxies are the first to form their stars and populate the mass function, being in place at $z \sim 1$. This is the called "downsizing" scenario [14]: massive galaxies experienced most of their star formation at early times and were passive by $z \sim 1$, and many among the less massive galaxies experienced extended star-formation histories [8, 23]. These results are a challenge to the popular hierarchical Λ-CDM models, in which one expects that the more massive dark matter halos were the final stage of successive mergers of smaller halos. However, the treatment of the barionic component is still unclear and its only accessible via semi-analytical models [6, 16]. In this framework, the role of the galaxy mergers in the buildup of the red sequence and its relative importance in the evolution of the galactic properties, e.g., colour, mass, or morphology, is an important open question.

The galaxy merger fraction, $f_{\rm m}$, defined as the number of merger galaxies in a sample, is an useful direct observational quantity to answer that question. Many works have determined the galaxy merger fraction and its evolution with redshift, usually parameterised as $f_{\rm m}(z) = f_{\rm m}(0)(1+z)^m$, using different sample selection and methods, like morphological criteria [9, 13, 22], kinematic close companions [19, 17], spatial close pairs [18, 7] or correlation function [4]. In these works the value of the merger index varies in the range $m = 0 - 4$. Λ-CDM models predict $m \sim 3$ [15] for dark matter halos, while semi-analytical models suggest a weak evolution, $m \sim 0 - 1$, for the galaxy merger fraction [5, 1].

In this paper we summarise preliminary results about the redshift evolution of the morphological merger fraction, $f_{\rm m}^{\rm mph}$, in B-band luminosity and mass samples up to z ~ 1 in SPITZER/IRAC-selected samples in GOODS-S area. We use $H_0 = 70$ Km s^{-1} Mpc^{-1}, $\Omega_M = 0.3$, and $\Omega_\Lambda = 0.7$ throughout. All magnitudes are Vega unless noted otherwise.

2 Data

Galaxies were selected from the merged photometric catalogue of SPITZER / IRAC selected sources in GOODS-S published by [23]. This catalogue has 9676 IRAC sources detected in 225 arcmin^2. The catalogue is 75% complete down to [3.6] $\sim$ 23.5 (AB), and includes spectroscopic redshifts and photometric data in a variety of bands from the UV to the MIR, including GALEX (UV), HST/ACS ($F435W, F606W, F775W, F850LP$), VLT/ISAAC ($J, H, K$), SPITZER/IRAC (3.6, 4.5, 5.4, 8.5 μm), SPITZER/MIPS (24 μm), CHANDRA (X-Ray) and COMBO-17 filters. We have used the photometric redshifts, absolute magnitudes and stellar masses presented in [23]. For details on the data set, see `http://t-rex.fis.ucm.es/~pgperez/Proyectos/databaseuse.en.html`. We took two different samples to study the merger

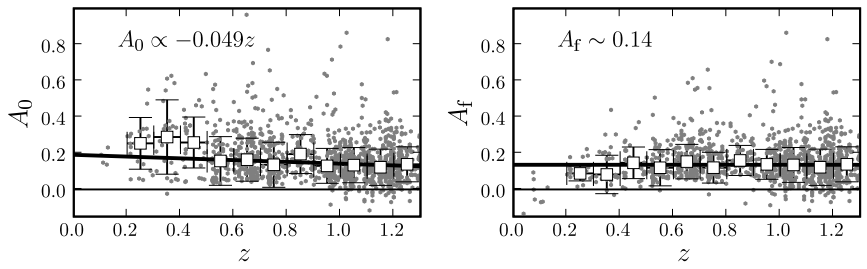

Fig. 1 Asymmetry vs. redshift in the $M_B \leq -20$ sample (*grey dots* in both panels). *Left*: asymmetries of the sources measured on the original images. *Right*: asymmetries of the sources measured on images degraded to $z_\mathrm{d} = 0.1$. White squares in both panels are the mean asymmetries in 0.1 redshift bins. The black solid line is the least-squares linear fit to the mean asymmetries in [0.5,1.3) redshift interval.

fraction evolution: one comprises the 1122 sources with $M_B \leq -20$, while other comprises the 982 with $M_\star > 10^{10}\ M_\odot$.

3 Asymmetry index

The automatic asymmetry index A is one of the CAS morphological indices [10]. It is defined as:

$$A = \frac{\sum |I_0 - I_{180}|}{\sum |I_0|} - \frac{\sum |B_0 - B_{180}|}{\sum |I_0|}, \tag{1}$$

where I_0 and B_0 are the original galaxy and background images, I_{180} and B_{180} are the original galaxy and background images rotated by 180 degrees, and the sum spans all the pixels of the galaxy and background images. For further details on the asymmetry calculation see [12]. We use the A index to identify recent merger systems which are very distorted. On the basis of asymmetry measurements on images of nearby merger remnants, previous merger fraction determinations have taken a system to be a major merger remnant if its asymmetry index is $A > A_\mathrm{m}$, with $A_\mathrm{m} = 0.35$ [10]. Note that this criterion applies to disk-disk mergers only. For high-redshift samples the determination of A needs to be done on HST images to ensure high spatial resolution. In our work, and to avoid morphological K-corrections [9], we determined the asymmetry in $F435W$ image where the source has $0 < z \leq 0.15$, in $F606W$ image where $0.15 < z \leq 0.55$, in $F775W$ image where $0.55 < z \leq 0.9$, and in $F850LP$ image where $0.9 < z \leq 1.3$.

The asymmetry index measured on survey images systematically varies with the source redshift due to the loss of spatial resolution and source flux descent with z. The net result is a systematic decrease with z of the mea-

sured asymmetry. In our work we treated this bias by degrading all the source images to a representative common redshift, which we chose as $z_{\rm d} = 1$. The degradation procedure is explained in detail in [21]. The degradation of the images was done with COSMOSHIFT [3], which performs repixelation, PSF change, and flux decrease over the sky-subtracted source image. The final obtained asymmetries referred to $z_{\rm d} = 1$, $A_{\rm f}$, provide a homogeneous asymmetry set that permits consistent morphological studies in GOODS-S field.

How does degradation affect local merger criterion $A > A_{\rm m} = 0.35$? We assume that $A_{\rm m}(z) = A_{\rm m}(0) + \delta_A z = 0.35 + \delta_A z$, where degradation rate δ_A is the statistical descent of asymmetry with redshift for luminosity or mass sample. We determine δ_A by comparing the tendency of the initial asymmetry A_0 (i.e., measured in non-degraded images) and the final asymmetry $A_{\rm f}$ with redshift. In the left panel of Figure 1 we show the variation of A_0 with redshift in the $M_B \leq -20$ sample, while in the right panel we see the variation of $A_{\rm f}$ for the same sample. In both panels white squares are the median asymmetries in $\Delta(z) = 0.1$ redshift bins and the black solid line is the least-squares linear fit to the $0.5 \leq z < 1.3$ points. In the A_0 case the slope of the fit is negative, $A_0 \propto -0.049z$, while in the $A_{\rm f}$ case the slope is null, $A_{\rm f} \sim 0.14$. In the first case, the negative slope reflects that the loss of information with redshift (negative effect on A) dominates over genuine population variations. In the second case, we have removed the loss of information term, so we only see population effects. We take as degradation rate the difference between both slopes, that yields $\delta_A = -0.05$. We follow the same procedure in the mass sample, obtaining a similar degradation rate. Finally, we take $A_{\rm m}(1) = 0.35 - 0.05 = 0.3$.

4 Merger fraction determination by maximum likelihood method

Following [11], the merger fraction by morphological criteria is $f_{\rm m}^{\rm mph} = N_{\rm m}/N_{\rm tot}$, where $N_{\rm m}$ is the number of the distorted sources in the sample with $A > A_{\rm m}$, and $N_{\rm tot}$ is the total number of sources in the sample.

The steps that we follow to obtain the merger fraction are described in detail in [20], so we only review the main steps. If we define a bidimensional histogram in the redshift–asymmetry space and normalise this histogram to unity, we obtain a bidimensional probability distribution defined by the probability of having one source in bin $[z_k, z_{k+1}) \cap [A_l, A_{l+1})$, defined as p_{kl}, where index k spans the redshift bins of size Δz, and the index l spans the asymmetry bins of size ΔA. We consider only two asymmetry bins split at $A_{\rm m}$, such that the probabilities p_{k1} describe highly distorted galaxies (i.e., merger systems), while the probabilities p_{k0} describe normal galaxies. With those definitions, the merger fraction in the redshift interval $[z_k, z_{k+1})$ becomes

$$f_{\mathrm{m},k}^{\mathrm{mph}} = \frac{p_{k1}}{p_{k0} + p_{k1}}. \quad (2)$$

In reference [20] we developed a maximum likelihood (ML) method that yields the most probable values of p_{kl} taking into account not only the z and A values, but also their experimental errors. In addition, the ML method provides an estimate of the 68% confidence intervals of the probabilities p_{kl}, that we use to obtain the $f_{\mathrm{m},k}^{\mathrm{mph}}$ 68% confidence intervals. Reference [20] shows, using synthetic catalogues, that the experimental errors tend to smooth an initial bidimensional distribution described by p_{kl}, due to spill-over of sources to neighbouring bins. This leads to a $\sim 30-50\%$ overestimate of the galaxy merger fraction in typical observational cases. In addition, thanks to the use of the ML method we accurately recover the initial bidimensional distribution: the input and ML method merger fraction difference is $\sim 1\%$ even when experimental errors are as large as to the bin size.

5 Results

We summarise our merger fractions in Table 1. Our principal results are:

1. We obtain low morphological merger fractions, $f_{\mathrm{m}}^{\mathrm{mph}} < 0.06$ up to $z \sim 1$.
2. The merger fraction in mass sample is lower than in luminosity sample, in agreement with previous near infrared studies [7, 24, 21].
3. The merger fraction evolution is very different in the two samples: $f_{\mathrm{m}}^{\mathrm{mph}}(z, M_B \leq -20) = 0.013(1+z)^{1.8}$, while $f_{\mathrm{m}}^{\mathrm{mph}}(z, M_\star > 10^{10}\ M_\odot) = 0.001(1+z)^{5.4}$ (left panel in Figure 2).
4. Following [19], we find that the disk-disk major merger remnant fraction since $z = 1$ is $f_{\mathrm{rem}} = 20\%\pm5\%$ for $M_B \leq -20$ galaxies and $f_{\mathrm{rem}} = 8\%\pm3\%$ for $M_\star > 10^{10}\ M_\odot$ galaxies.
5. Combining our intermediate redshift merger fractions for $M_\star > 10^{10}\ M_\odot$ galaxies with those from [13] at $1 < z < 2.5$ in the same mass range, we conclude that the power-law parameterisation is only valid for $z < 1.5$. A mixed power law-exponential function, $0.00034(1+z)^{10.5}\mathrm{e}^{-0.57(1+z)^2}$, is a better parameterisation up to $z \sim 2.5$.
6. With the previous parameterisation we infer that a $M_\star > 10^{10}\ M_\odot$ galaxy suffer in average $1.2^{+0.4}_{-0.3}$ disk-disk major mergers since $z \sim 3$. Interestingly, almost all merger activity occurs at $z > 1$, $1.0^{+0.4}_{-0.2}$, with only 0.2 disk-disk major mergers in $0 < z < 1$ (right panel in Figure 2). This result suggests that disk-disk major mergers are not an important process in galactic evolution since $z \sim 1$, but they may be important at higher redshifts.

Acknowledgements This work was supported by the Spanish Programa Nacional de Astronomía y Astrofísica through project number AYA2006-12955.

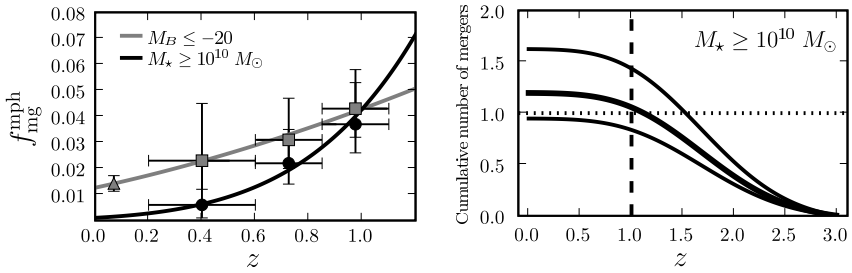

Fig. 2 *Left*: Morphological merger fraction in function of redshift for $M_B \leq -20$ (*grey squares*) and $M_\star \geq 10^{10}\ M_\odot$ galaxies (*black dots*). The grey/black solid line is the least-squares fit of the data to $f_{\rm m}^{\rm mph}(z) = f_{\rm m}^{\rm mph}(0)(1+z)^m$ in the luminous/mass case, respectively. The grey triangle is the $M_B \leq -20$ estimation from [21] of the [17] $M_B \leq -19$ merger fraction. *Right*: Cumulative number of disk-disk major mergers per galaxy since $z \sim 3$. Solid lines are the mean number of mergers and its uncertainty. Dashed line marks $z = 1$, while dots line marks one cumulative merger per galaxy since $z \sim 3$.

Table 1 Morphological major merger fractions $f_{\rm m}^{\rm mph}$ in GOODS-S

Sample selection	z = 0.4	z = 0.725	z = 0.975	$f_{\rm m}^{\rm mph}(0)$	m
$M_B \leq -20$	$0.023^{+0.022}_{-0.011}$	$0.031^{+0.016}_{-0.011}$	$0.043^{+0.015}_{-0.011}$	0.013 ± 0.003	1.8 ± 0.5
$M_\star \geq 10^{10}\ M_\odot$	$0.006^{+0.018}_{-0.005}$	$0.022^{+0.013}_{-0.008}$	$0.037^{+0.016}_{-0.011}$	$(1.0 \pm 0.2) \times 10^{-3}$	5.4 ± 0.4

References

1. M. Abilio: ArXiv e-prints, 0802.2720 (2008)
2. R. G. Abraham et al: MNRAS, **279**, L47 (1996)
3. M. Balcells, D. Cristóbal-Hornillos, & M. C. Eliche-Moral: RMxAA Conference Series, **16**, 259 (2003)
4. E. F. Bell et al.: ApJ, **652**, 270 (2006)
5. J. C. Berrier: ApJ, **652**, 56 (2006)
6. R. G. Bower, et al.: MNRAS, **370**, 645 (2006)
7. K. Bundy et al.: ApJ, **601**, L123 (2004)
8. K. Bundy et al.: ApJ, **651**, 120, (2006)
9. P. Cassata et al.: MNRAS, **357**, 903 (2005)
10. C. J. Conselice: ApJS, **147**, 1 (2003)
11. C. J. Conselice: ApJ, **638**, 686 (2006)
12. C. J. Conselice, M. A. Bershady, A. Jangen: ApJ, **529**, 886 (2000)
13. C. J. Conselice, R. Sheena, & R. Myers: MNRAS, **386**, 909 (2008)
14. L. L. Cowie et al.: AJ, **112**, 839 (1996)
15. S. Gottlöber, A. Klypin, A. V. Kravtsov: ApJ, **546**, 223 (2001)
16. G. De Lucia & J. Blaizot: MNRAS, **375**, 2 (2007)
17. R. De Propris et al.: ApJ, **666**, 212 (2007)
18. O. Le Fèvre, O. et al.: MNRAS, **311**, 565 (2000)
19. D. R. Patton et al.: ApJ, **536**, 153 (2000)
20. C. López-Sanjuan, C. E. García-Dabó, M. Balcells: PASP, **120**, 571 (2008)
21. C. López-Sanjuan et al.: ApJ submitted (2008)
22. J. M. Lotz et al.: ApJ, **672**, 177 (2008)
23. P. G. Pérez-González et al.: ApJ, **675**, 234 (2008)
24. A. Rawat et al: ApJ, **681**, 1089 (2008)